

Original Article
Microbiology



C1qa deficiency in mice increases susceptibility to mouse hepatitis virus A59 infection

Han-Woong Kim ^{1,2}, Sun-Min Seo ¹, Jun-Young Kim ^{1,3}, Jae Hoon Lee ⁴,
Han-Woong Lee ⁴, Yang-Kyu Choi ^{1,*}

¹Department of Laboratory Animal Medicine, College of Veterinary Medicine, Konkuk University, Seoul 05029, Korea

²Regenerative Dental Medicine Institute, Hysensbio, Gwacheon 13814, Korea

³Green Cross Corporation, Yongin 16924, Korea

⁴Department of Biochemistry, College of Life Science and Biotechnology, Yonsei University, Seoul 03722, Korea

 OPEN ACCESS

Received: Sep 1, 2020

Revised: Jan 26, 2021

Accepted: Apr 15, 2021

*Corresponding author:

Yang-Kyu Choi

Department of Laboratory Animal Medicine,
College of Veterinary Medicine, Konkuk
University, 120 Neungdong-ro, Gwangjin-gu,
Seoul 05029, Korea.
E-mail: yangkyuc@konkuk.ac.kr


© 2021 The Korean Society of Veterinary
Science

This is an Open Access article distributed
under the terms of the Creative Commons
Attribution Non-Commercial License (<https://creativecommons.org/licenses/by-nc/4.0>)
which permits unrestricted non-commercial
use, distribution, and reproduction in any
medium, provided the original work is properly
cited.


ORCID iDs

Han-Woong Kim 


<https://orcid.org/0000-0001-7542-3575>

Sun-Min Seo 

<https://orcid.org/0000-0001-7543-846X>

Jun-Young Kim 


<https://orcid.org/0000-0002-4948-6860>

Jae Hoon Lee 

<https://orcid.org/0000-0001-9777-5918>

Han-Woong Lee 

<https://orcid.org/0000-0001-9515-3605>

Yang-Kyu Choi 

<https://orcid.org/0000-0002-4969-5443>

ABSTRACT

Background: Mouse hepatitis virus (MHV) A59 is a highly infectious pathogen and starts in the respiratory tract and progresses to systemic infection in laboratory mice. The complement system is an important part of the host immune response to viral infection. It is not clear the role of the classical complement pathway in MHV infection.

Objectives: The purpose of this study was to determine the importance of the classical pathway in coronavirus pathogenesis by comparing *C1qa* KO mice and wild-type mice.

Methods: We generated a *C1qa* KO mouse using CRISPR/Cas9 technology and compared the susceptibility to MHV A59 infection between *C1qa* KO and wild-type mice. Histopathological and immunohistochemical changes, viral loads, and chemokine expressions in both mice were measured.

Results: MHV A59-infected *C1qa* KO mice showed severe histopathological changes, such as hepatocellular necrosis and interstitial pneumonia, compared to MHV A59-infected wild-type mice. Virus copy numbers in the olfactory bulb, liver, and lungs of *C1qa* KO mice were significantly higher than those of wild-type mice. The increase in viral copy numbers in *C1qa* KO mice was consistent with the histopathologic changes in organs. These results indicate that *C1qa* deficiency enhances susceptibility to MHV A59 systemic infection in mice. In addition, this enhanced susceptibility effect is associated with dramatic elevations in spleen IFN- γ , MIP-1 α , and MCP-1 in *C1qa* KO mice.

Conclusions: These data suggest that *C1qa* deficiency enhances susceptibility to MHV A59 systemic infection, and activation of the classical complement pathway may be important for protecting the host against MHV A59 infection.

Keywords: Mouse hepatitis virus; classical complement pathway; knockout mouse; CRISPR

INTRODUCTION

Mouse hepatitis virus (MHV) constitutes a group of betacoronaviruses and is commonly used as a model to study coronavirus entry, replication, and pathogenesis [1,2]. Many MHV strains can infect laboratory mice. MHV may be transmitted by aerosols, fomites, or direct contact

Funding

This paper was supported by Konkuk University in 2018.

Conflict of Interest

The authors declare no conflicts of interest.

Author Contributions

Conceptualization: Lee HW, Choi YK. Data curation: Seo SM. Formal analysis: Kim HW, Seo SM. Funding acquisition: Lee HW, Choi YK. Investigation: Kim HW, Seo SM. Methodology: Kim HW, Kim JY, Lee JH. Project administration: Seo SM, Kim JY. Resources: Kim HW, Seo SM. Software: Kim HW, Kim JY, Lee JH. Supervision: Lee HW, Choi YK. Validation: Seo SM, Lee JH. Visualization: Kim HW, Kim JY. Writing - original draft: Kim HW. Writing - review & editing: Choi YK.

[3,4]. There are two major strains of MHV: polytropic strains, which are primarily spread by aerosols or fomites, and enterotropic strains, which are transmitted through ingestion of fecal material from infected mice [5]. Generally polytropic strains such as MHV A59, MHV-1, JHM can cause systemic infections.

The activation of complement system is a critical mechanism for the host to defend against many bacterial, viral, and fungal infections. It is involved with pattern recognition receptors to stimulate host defense systems prior to activation of the adaptive immune response [6]. Complement component 1q (C1q) is a protein complex involved in the classical pathway of the complement system, which is part of the innate immune system [7]. C1q binds to the surface of the pathogen, C-reactive protein, or Fc region of the antibody that binds to an antigen. Subsequently, the classical pathway is initiated by forming the C1 complex with the serine protease subunits C1r and C1s [8]. Among the three complement pathways, mice with no *C1qa* gene experience a blocked classical pathway while the lectin and alternative pathways proceed normally [9]. Hereditary deficiency in the C1q protein is associated with absence of the classical pathway, which leads to the development of systemic lupus erythematosus [10]. Approximately 25% of the *C1qa* knockout mice in one study developed glomerulonephritis at 8 months of age, and mice without glomerulonephritis showed more glomerular apoptotic bodies compared to wild-type mice [9]. C1q binds to apoptotic keratinocytes in an antibody-independent pattern. In C1q deficiency, where the removal of apoptotic cells is abnormal, these keratinocytes may provide a major source of autoantigens that drive the innate immune response in systemic lupus erythematosus and related autoimmune diseases [11].

Previous study of *C1qa*-deficient mice has demonstrated that the classical complement pathway is required for innate immunity to *Streptococcus pneumoniae* infection in mice [12]. However, the mechanisms of *C1qa*-associated responses in coronavirus infection are not well known. In this study, we generated a *C1qa* knockout mouse using CRISPR/Cas9 technology to study susceptibility to MHV A59 infection. The purpose of this study was to determine the importance of the classical pathway in coronavirus pathogenesis by comparing *C1qa* KO mice and wild-type mice.

MATERIALS AND METHODS

Cell and virus stock preparation

A mouse fibroblast cell line (NCTC clone 929, KCLB-10001, Korea) was cultivated in Dulbecco's modified eagle medium supplemented with 10% fetal bovine serum. The MHV A59 strain (ATCC® VR-550™, USA) was inoculated after approximately 70–80% confluency. After 5 days of inoculation, the culture flask was frozen at -70°C and then thawed at room temperature. Cell lysate was centrifuged at $3,000 \times g$, and the resulting supernatant was filtered with a $0.25 \mu\text{m}$ syringe filter. The viral stock was divided into $500 \mu\text{L}$ aliquots and stored at -70°C . The virulence of the harvested viral stock was measured by endpoint dilution assay. The viral titer was determined to be 1×10^7 TCID₅₀/mL.

Animal experiment

C57BL/6J-*C1qa* knockout (*C1qa* KO) mice were generated using CRISPR/Cas9 technology at Yonsei University (Seoul, Republic of Korea) as described previously [13]. *C1qa* KO and C57BL/6J (wild-type) mice were raised in the laboratory animal breeding room at the College of Veterinary Medicine, Konkuk University (Seoul, Republic of Korea). The targeted

genotypes of *C1qa* KO and wild-type mice were confirmed by polymerase chain reaction (PCR) amplification of genomic DNA extracted from tail biopsies (**Supplementary Fig. 1**). Specific pathogen-free conditions were maintained in the breeding room. The mice were housed individually in ventilated cages with sterilized feed, water, and bedding material. The temperature was maintained at $22 \pm 2^\circ\text{C}$ by air-conditioning facilities, and the humidity was kept at $50 \pm 10\%$ with a 12 h light/dark cycle. All animal studies were approved by the Institutional Animal Care and Use Committee of Konkuk University (KU19100).

Virus inoculation

Four-week-old *C1qa* KO and wild-type mice were anesthetized with Alfaxalone (60 mg/kg) and Xylazine (5 mg/kg) intraperitoneally. The virus stock was diluted with phosphate-buffered saline (PBS). After confirming the loss of pain sensation, 5×10^3 TCID₅₀ of MHV A59 was inoculated intranasally. Clinical signs and body weight changes were observed and documented daily. Infected mice in each group (n = 5) were sacrificed on both days 3 and 6 post-infection. The weights of the liver, lungs, and spleen were measured to compare the organ to body weight ratio. Susceptible organs, such as the brain, liver, lungs, spleen, and intestines, were harvested for molecular and histopathologic analyses. Parts of the organ samples were fixed in 10% neutral-buffered formalin for paraffin section, and the rest were frozen at -80°C .

Quantification of viral copy number in each organ

Primers were designed to detect the MHV A59 nucleocapsid (N) gene, which is comprised of 157 base pairs (bp). The forward primer was 5'-GCGTTGCAAAGCCCA-3', and the reverse primer was 5'-CGCCGACATAGGATTCAT-3'. The brain, spinal cord, liver, lungs, spleen, and ileum were isolated from infected mice. The brain was separated into the olfactory bulb, cerebrum, and cerebellum. Each organ (20 mg) was homogenized and centrifuged at $3,000 \times g$. Viral RNA was isolated using the Viral Gene-spin Viral DNA/RNA Extraction Kit (iNtRON Biotechnology, Republic of Korea). For cDNA synthesis, the mixture of extracted RNA was incubated at 60°C for 15 min and immediately cooled on ice. The standard curve was generated using 10-fold serial dilutions of the purified cDNA. The dilution ranged from 10^9 to 10^1 copies/uL and was tested in triplicate. The standard curve was plotted between the standard DNA concentration (log copy number) and threshold cycle (Ct). Ct values in susceptible organ tissues were measured by real-time PCR (RT-PCR), and viral copy numbers per mg of organ were calculated by extrapolating the average Ct values from the standard curve. RT-PCR was conducted with the CFX96 real-time system (Bio-Rad, USA) and AccuPower GreenStar RT-qPCR Master Mix (Bioneer, Korea) according to each manufacturer's recommendations.

Quantitative RT-PCR in the spleen

mRNA was isolated from the spleen of *C1qa* KO and wild-type mice to compare the expression levels of cytokines and chemokines, such as IFN- α , IFN- β , IFN- γ , IL-6, macrophage inflammatory protein-1 α (MIP-1 α), and monocyte chemoattractant protein-1 (MCP-1). mRNA isolation was accomplished using TRIzol reagent (Ambion, Inc., USA), and cDNA was synthesized using M-MLV reverse transcriptase (Invitrogen). RT-PCR was conducted with the CFX96™ real-time system (BIO-RAD) using AccuPower GreenStar RT-qPCR Master Mix (Bioneer) according to each manufacturer's recommendations. The RT-PCR primers used are shown in **Table 1**. The Ct value of each gene, which is inversely correlated with the expression level, was measured as the cycle number at which fluorescent emission increased above a certain threshold. The relative expression of each sample was normalized to the expression of β -actin, the housekeeping gene, and calculated by the $2^{-\Delta\Delta\text{Ct}}$ method.

Table 1. The primer sequences of cytokine and chemokine

Gene	RT-PCR primers
<i>β-actin</i>	Forward 5'-GCGAGCACAGCTTCTTTGCAGC-3' Reverse 5'-AATACAGCCCGGGGAGCATCGT-3'
<i>lfn-α</i>	Forward 5'-GGACTTTGGATCCCCGAGGAGAAG-3' Reverse 5'-GCTGCATCAGACAGCCTTGCAAGTC-3'
<i>lfn-β</i>	Forward 5'-AACCTCACCTACAGGGCGGACTTCA-3' Reverse 5'-TCCACGTCATCTTCTCTTGCTTT-3'
<i>lfn-γ</i>	Forward 5'-TCAAGTGGCATAGATGTGGAAGAA-3' Reverse 5'-TGGCTCTGCAGGATTTTCATG-3'
<i>Il-6</i>	Forward 5'-GAGGATAACCACTCCCAACAGACC-3' Reverse 5'-AAGTGCATCATCGTTGTCATACA-3'
<i>MCP-1</i>	Forward 5'-CTTCTGGGCTGCTGTCA-3' Reverse 5'-CCAGCCTACTCATTGGGATCA-3'
<i>MIP-1α</i>	Forward 5'-CTTCTGTACCATGACACTC-3' Reverse 5'-AGGTCTTTGGAGTCAGCG-3'

Histopathological analysis

The brain, lungs, liver, and intestines were removed from sacrificed mice, fixed with 10% neutral-buffered formalin, and processed for paraffin section. Next, each organ was embedded in paraffin and cut into 5 μm thick sections. The sections were deparaffinized, rehydrated, and stained with hematoxylin and eosin. After staining, the sections were examined under a BX51 light microscope (Olympus, Japan), and the images were captured by DP71 software (Olympus). To quantify histopathological lesions, the left lateral lobe, right median lobe, and quadrate lobe of the liver were assessed in the 200× field of view under the following parameters: 0: normal; 1: infiltration of focal inflammatory cells; 2: hepatocellular necrosis containing less than approximately 25% of the liver; 3: hepatocellular necrosis containing less than approximately 50% of the liver; 4: hepatocellular necrosis containing less than approximately 75% of the liver; and 5: hepatocellular necrosis containing more than approximately 75% of the liver. The total score of the liver was determined by 3 researchers, and three sites were analyzed.

Immunohistochemistry

Samples were cut into 5 μm thick sections on silane-coated slide glass. Antigen retrieval was accomplished by using 0.1 M sodium citrate in a microwave oven. Slides were cooled at room temperature, and endogenous peroxidase activity was inhibited with 3% hydrogen peroxide. M.O.M. IgG Blocking Reagent (Vector Laboratories, USA) was used to minimize non-specific reactions. MHV A59 was detected using the monoclonal antibody to MHV NSP9 (OriGene Technologies Inc., USA). Biotinylated Anti-Mouse IgG Reagent (Vector Laboratories) was used as the secondary antibody, and detection was conducted using the DAB Peroxidase Substrate Kit (Vector Laboratories). All slides were counterstained with hematoxylin.

Statistical analysis

Statistically significant differences between the two groups were evaluated by the two-tailed Student's *t*-test. A *p*-value less than 0.05 was determined to be statistically significant. All values are expressed as means ± SE. The virus copy number of each sample was calculated using the following formula from the standard curve plotted between the log copy number and Ct value [14]:

$$DNA\ copy\ number = 10^{\frac{38.567 - Ct}{3.6549}}$$

RESULTS

Body weight changes

Body weight was lost in both *C1qa* KO and wild-type mice from day 1 of MHV A59 infection. *C1qa* KO mice continued to lose weight until the end of the experiment while wild-type mice recovered weight from day 4 post-infection (**Fig. 1A**). Body weight change (%) in *C1qa* KO mice was significantly ($p < 0.05$) lower than that of wild-type mice between days 4 and 6 post-infection. On the 6th day after infection, the body weight loss rate was approximately 16% in *C1qa* KO mice, but there were no cases of death in either group.

Organ to body weight ratios

Organ weights of the liver, lungs, and spleen were measured on both days 3 and 6 after infection in each group. The liver to body weight ratio in *C1qa* KO mice on day 6 post-infection was significantly ($p < 0.05$) higher than that of the other 3 groups (**Fig. 1B**). On the sixth day post-infection, the lung to body weight ratio was significantly increased in *C1qa* KO mice compared to wild-type mice (**Fig. 1C**). Both *C1qa* KO and wild-type mice showed a significantly higher ratio of the spleen to body weight on day 6 relative to day 3 after infection (**Fig. 1D**). The spleen to body weight ratio in *C1qa* KO mice on day 6 post-infection was increased compared to wild-type mice; however, there was no significant difference between the two groups.

Viral loads in susceptible organs

Virus copy numbers of MHV A59 in organs were measured by RT-PCR. Both *C1qa* KO and wild-type mice showed a significant increase in viral load in infected organs. In the olfactory

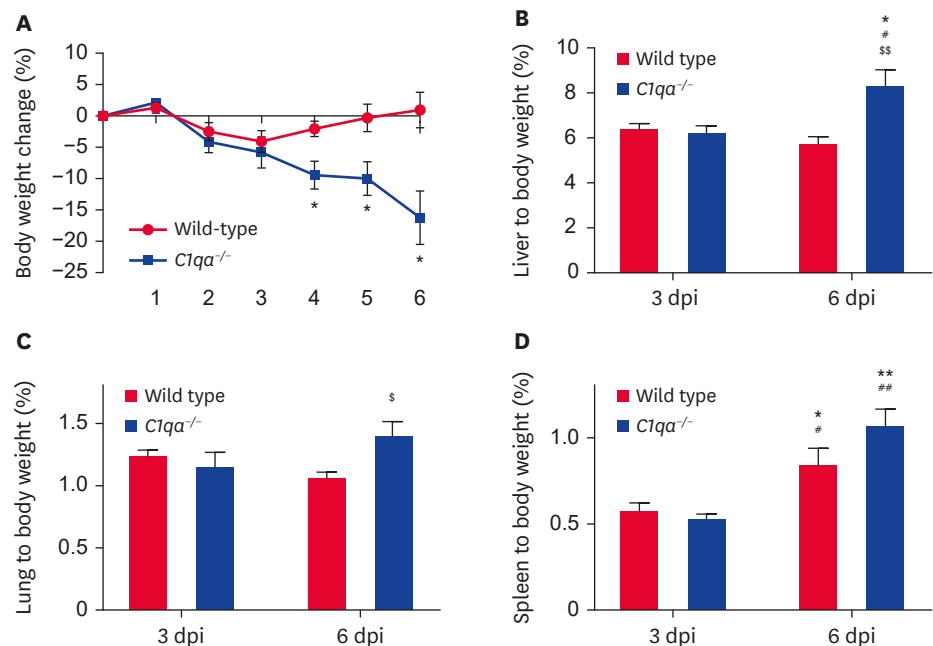


Fig. 1. Body weight changes and organ to body weight ratios in *C1qa* knockout (*C1qa*^{-/-}) and wild-type mice. All mice in each group ($n = 5$) were inoculated intranasally with 5×10^5 TCID₅₀ of mouse hepatitis virus (MHV) A59. (A) Body weights were measured daily until the end of the experiment. * $p < 0.05$ versus wild-type mice at the indicated time points. Organ to body weight ratios in the liver (B), lungs (C), and spleen (D) both 3 and 6 dpi were calculated. Data are presented as means \pm SE. * $p < 0.05$, ** $p < 0.01$ versus 3 dpi of wild-type; # $p < 0.05$ and ** $p < 0.01$ versus 3 dpi of *C1qa*^{-/-}; ^s $p < 0.05$ and ** $p < 0.01$ versus 6 dpi of wild-type. dpi, days post-infection.

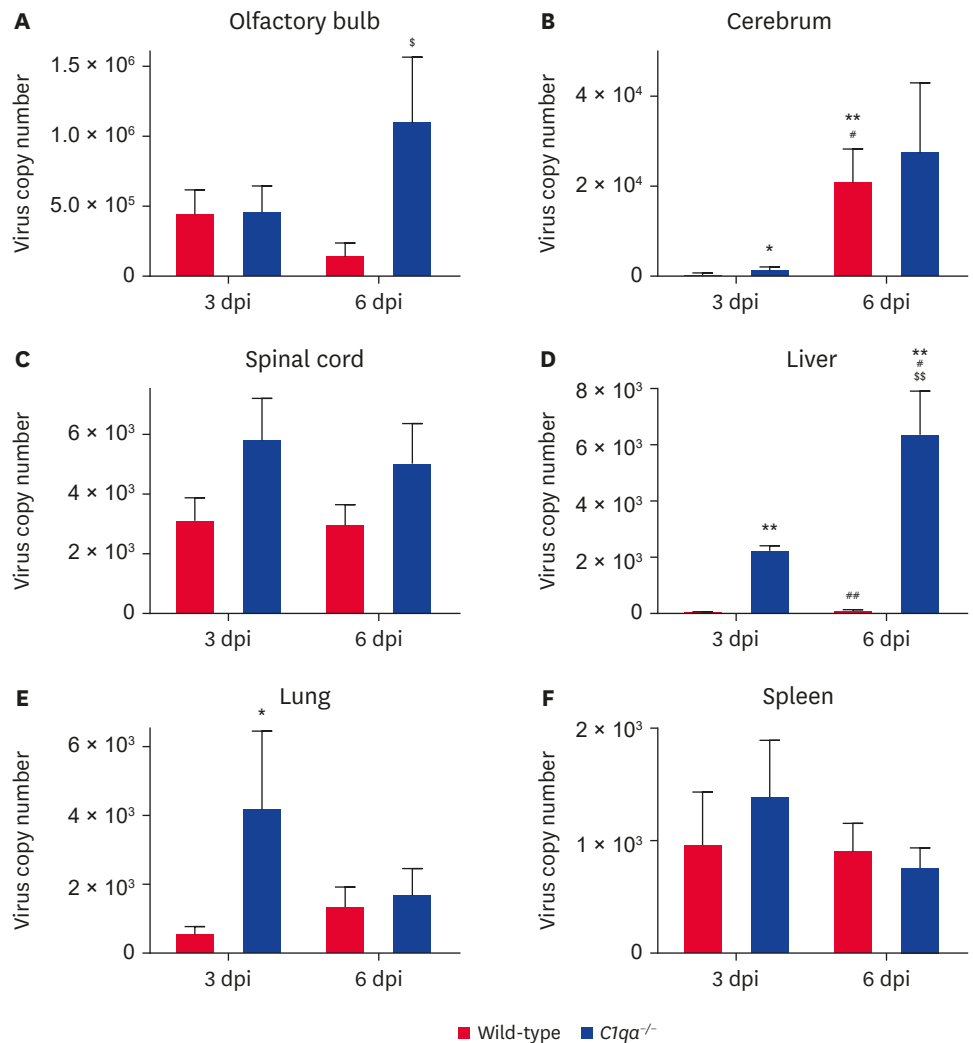


Fig. 2. Virus copy numbers in *C1qa* knockout (*C1qa*^{-/-}) and wild-type mice. All mice in each group (n = 5) were inoculated intranasally with 5×10^3 TCID₅₀ of mouse hepatitis virus (MHV) A59. Virus copy numbers per mg of tissue were measured from the olfactory bulb (A), cerebrum (B), spinal cord (C), liver (D), lungs (E), and spleen (F) both 3 and 6 dpi. Data are presented as means \pm SE. * $p < 0.05$, ** $p < 0.01$ versus 3 dpi of wild-type; # $p < 0.05$ and ## $p < 0.01$ versus 3 dpi of *C1qa*^{-/-}; \$ $p < 0.05$ and \$\$ $p < 0.01$ versus 6 dpi of wild-type. dpi, days post-infection.

bulb, virus copy numbers of *C1qa* KO mice on day 6 post-infection were significantly ($p < 0.05$) higher than that of wild-type mice (Fig. 2A). In the cerebrum, virus copy numbers of *C1qa* KO mice were higher than those of wild-type mice on day 3 after infection. Virus copy numbers in the cerebrum were increased in *C1qa* KO mice on day 6 post-infection compared to wild-type and *C1qa* KO mice on day 3 post-infection, but no significant difference was observed (Fig. 2B). In the spinal cord, virus copy numbers of *C1qa* KO mice were higher than those of wild-type mice on both days 3 and 6 after infection, but there was no statistically significant difference between the two groups (Fig. 2C). Virus copy numbers in the cerebellum were less than 400 copies/mg in all groups (data not shown). Among the central nervous system organs, the olfactory bulb had the highest viral load. The livers of *C1qa* KO mice on both days 3 and 6 after infection demonstrated a significant increase in virus copy numbers compared to those of wild-type mice. Virus copy numbers in the livers of *C1qa* KO mice were greatly increased on day 6 compared to day 3 post-infection (Fig. 2D). In the lungs, virus copy numbers of *C1qa* KO mice

on day 3 after infection were significantly higher than those of wild-type mice (**Fig. 2E**). Virus copy numbers in the spleen (**Fig. 2F**) and ileum (data not shown) were less than 2,000 copies/mg in all groups, and there was no statistically significant difference between groups. Aside from the central nervous system, the liver had the highest viral load. The most susceptible organ to MHV A59 infection in our study was the olfactory bulb.

Histopathology and immunohistochemistry

Single or multiple hepatocellular necrosis was observed in the livers of both *C1qa* KO and wild-type mice on day 3 after infection. Necrosis was accompanied by inflammatory cell infiltrates. By day 6 post-infection, multiple hepatocellular necrosis was enlarged and became confluent in both *C1qa* KO and wild-type mice (**Fig. 3A**). Hepatocellular necrosis

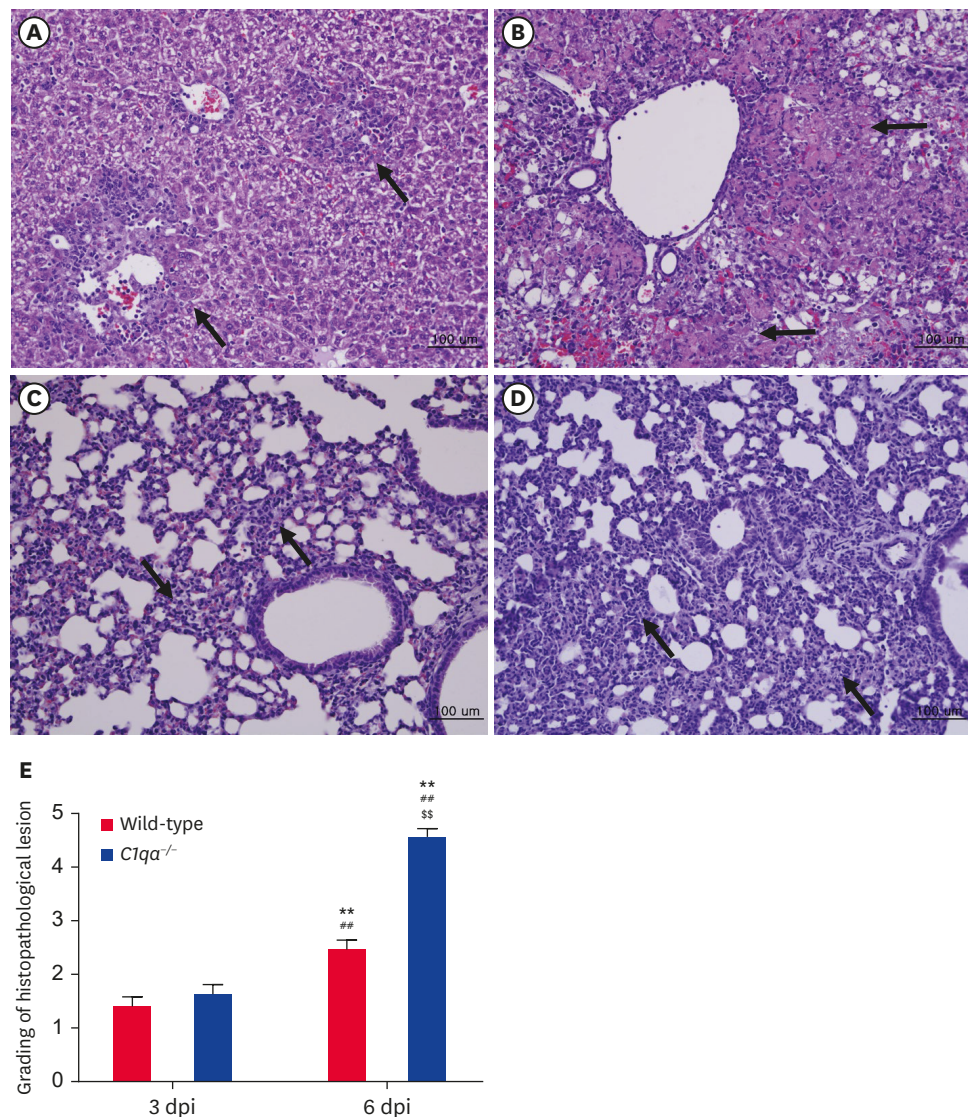


Fig. 3. Histopathological lesions in *C1qa* knockout (*C1qa*^{-/-}) and wild-type mice. Hepatocellular necrosis (arrows) was present in wild-type (A) and *C1qa* knockout (B) mice 6 dpi. Interstitial pneumonia with leukocyte infiltration (arrows) were present in the lungs of wild-type (C) and *C1qa* knockout (D) mice 6 dpi, respectively. Hematoxylin and eosin staining (A-D). (E) Hepatic histopathological changes were assessed and graded by 3 researchers. Data are presented as means \pm SE. ** $p < 0.01$ versus 3 dpi of wild-type; ## $p < 0.01$ versus 3 dpi of *C1qa*^{-/-}; \$\$ $p < 0.01$ versus 6 dpi of wild-type. dpi, days post-infection.

in *C1qa* KO mice on day 6 post-infection had extended throughout the entire liver (**Fig. 3B**). Hepatocellular syncytia, a hallmark of MHV infection, were present around necrotic foci in all infected mice. The livers of *C1qa* KO mice on day 6 post-infection displayed a significant increase in the grading of histopathological lesions compared to that of wild-type mice on both days 3 and 6 after infection. Furthermore, the grading of hepatic histopathological lesions of wild-type mice on day 6 post-infection was significantly higher than those of *C1qa* KO and wild-type mice on day 3 post-infection (**Fig. 3E**). In the lungs of wild-type mice on both days 3 and 6 after infection, the alveolar walls were thickening due to inflammatory leukocyte infiltration. The interstitial pneumonia observed in wild-type mice (**Fig. 3C**) was exacerbated in *C1q* KO mice on both days 3 and 6 post-infection (**Fig. 3D**). Perivascular edema and accumulation of inflammatory cells in the perivascular space were also seen in both *C1qa* KO and wild-type mice.

Immunohistochemistry was used in this study to detect the presence of MHV A59 in tissues. MHV antigens in the livers of MHV A59-infected mice were detected in and around hepatocellular necrotic foci in *C1qa* KO (**Fig. 4A**) and wild-type mice. In the lungs, a few inflammatory cells in the alveolar walls were positive for MHV A59 antigens in *C1qa* KO (**Fig. 4B**) and wild-type mice. A large number of MHV A59 antigens were found in the white pulp of the spleen in *C1qa* KO (**Fig. 4C**) and wild-type mice, and a few MHV A59 antigens were observed in neurons of the cerebral cortex in *C1qa* KO (**Fig. 4D**) and wild-type mice.

Cytokine and chemokine expression levels in the spleen

Cytokines and chemokines, such as IFN- α , IFN- β , IFN- γ , IL-6, MIP-1 α , and MCP-1, were measured by RT-PCR and normalized by the β -actin housekeeping gene. IFN- γ mRNA

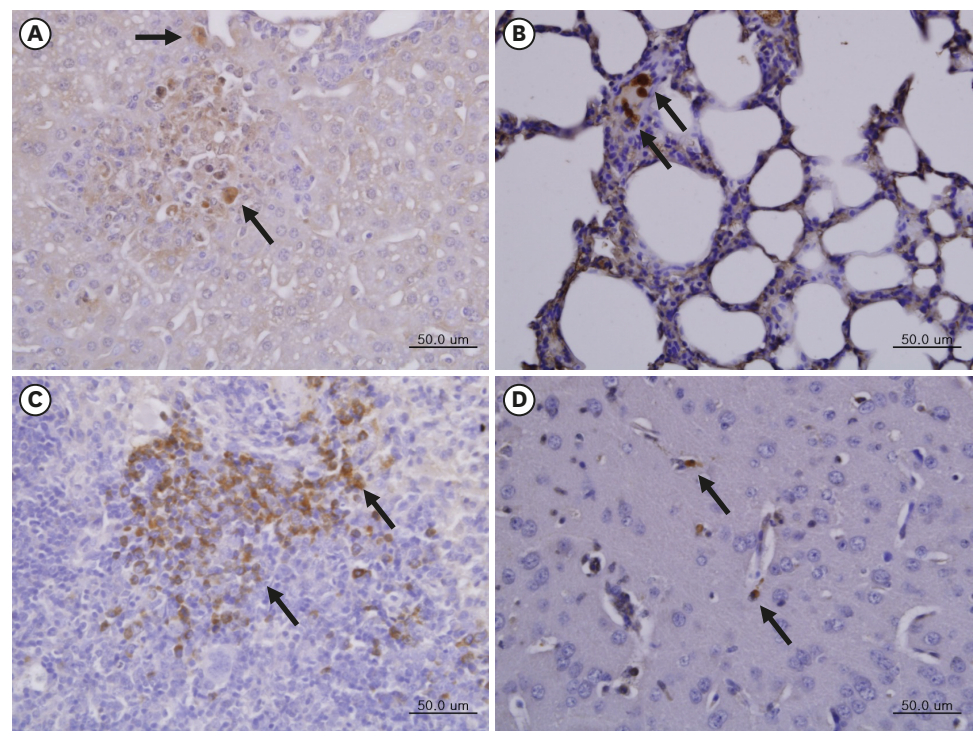


Fig. 4. IHC analysis in *C1qa* knockout mice. Mouse hepatitis virus A59 viral antigens (arrows) were present in the liver (A), lungs (B), white pulp of the spleen (C), and cerebral cortex (D) of *C1qa* knockout mice by IHC analysis. IHC, immunohistochemical.

expression levels in the spleens of *C1qa* KO mice at day 6 post-infection were significantly enhanced compared to those of the other 3 groups. In addition, IFN- γ expression levels in wild-type mice were significantly higher on day 6 relative to day 3 post-infection (**Fig. 5A**). The spleens of *C1qa* KO mice on day 6 post-infection displayed a significant increase in MIP-1 α mRNA expression levels compared to those of the other 3 groups. However, MIP-1 α expression levels in wild-type mice were significantly lower on day 6 relative to day 3 post-infection (**Fig. 5B**). MCP-1 mRNA expression was significantly upregulated by MHV A59 infection in *C1qa* KO mice compared to wild-type mice on both days 3 and 6 after infection (**Fig. 5C**). IL-6 mRNA expression levels on day 3 post-infection were slightly increased in *C1qa* KO mice compared to wild-type mice, but there was no significant difference between the two groups (**Fig. 5D**). IFN- α and IFN- β expression levels in *C1qa* KO mice on day 6 post-infection were higher than that of the other 3 groups, but there was no statistically significant difference between groups (**Fig. 5E and F**).

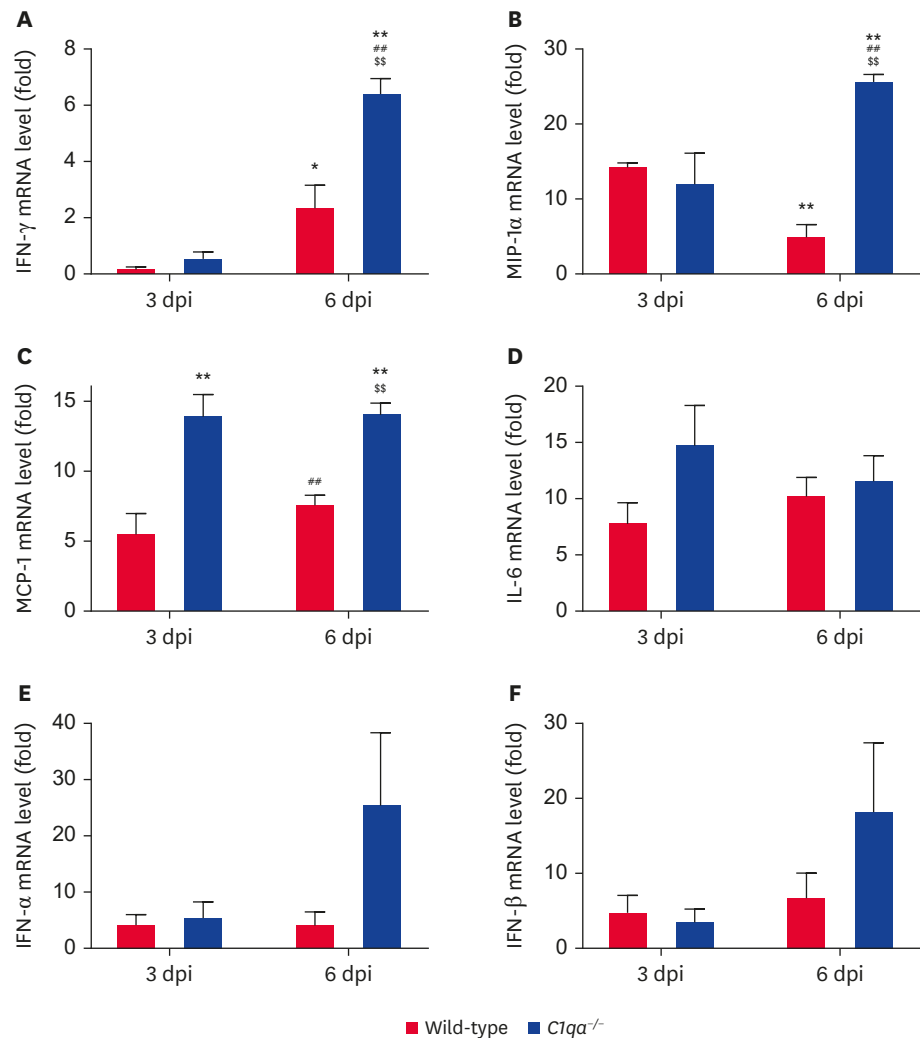


Fig. 5. Cytokine and chemokine mRNA expression levels in *C1qa* knockout (*C1qa*^{-/-}) and wild-type mice. IFN- γ (A), MIP-1 α (B), MCP-1 (C), IL-6 (D), IFN- α (E), and IFN- β (F) mRNA expression levels in the spleen were measured both 3 and 6 dpi by real-time polymerase chain reaction and normalized by the β -actin housekeeping gene. Data are presented as means \pm SE. * p < 0.05, ** p < 0.01 versus 3 dpi of wild-type; ## p < 0.01 versus 3 dpi of *C1qa*^{-/-}; \$\$ p < 0.01 versus 6 dpi of wild-type. dpi, days post-infection.

DISCUSSION

The activation of complement system is an important part of the host immune response to viral and bacterial infections. It has been known that viruses encode proteins to help them evade detection by the complement system [6,15], which means that this system plays an important role in the host antiviral response. However, the precise mechanisms of complement-associated responses in viral infections have not well been understood. Furthermore, given the three pathways in the complement system, it is not known what exact changes occur in the immune response against viral infections when each pathway is knocked out. Here, we investigated the susceptibility to MHV A59 infection using *C1qa* gene KO mice associated with the classical pathway. The *C1qa* KO mice used in this study were generated using CRISPR/Cas9 technology. Due to the ongoing threat and continued emergence of novel, highly contagious coronaviruses, a thorough understanding of host susceptibility to infection with MHV A59 will help to understand the pathogenesis of other coronaviruses.

To mimic natural infection, MHV A59 was inoculated in mice intranasally in this study. *C1qa* KO and wild-type mice were used to compare the difference in susceptibility to MHV A59 infection between normal and immunocompromised mice. The body conditions of infected mice were represented by body weight changes. From day 1 after infection, both *C1qa* KO and wild-type mice showed a decrease in body weight. Wild-type mice started to recover their weight from day 4 post-infection while *C1qa* KO mice gradually lost more weight until the end of the experiment. The continuous body weight loss after infection in *C1qa* KO mice was consistent with increases in viral loads. Viral loads in susceptible organs, such as the olfactory bulb, cerebrum, liver, and lungs, were significantly increased in *C1qa* KO mice compared to wild-type mice. Both *C1qa* KO and wild-type mice displayed histopathological lesions, such as hepatocellular necrosis, interstitial pneumonia, and perivascular inflammatory cell infiltrates, in the lungs. Histopathological lesions became more severe as MHV A59 infection progressed. When comparing wild-type mice, *C1qa* KO mice showed much more severe hepatitis and interstitial pneumonia in the lungs. These findings indicate that MHV A59 infection results in more severe viral loads as well as histopathological changes under *C1qa* deficiency. Since MHV A59 is a polytropic strain, MHV A59 antigens were detected in many organs, such as the liver, lungs, cerebrum, and spleen in both *C1qa* KO and wild-type mice by immunohistochemistry, as reported in previous studies [16-18]. The grade of histopathological lesions in the liver was much higher in *C1qa* KO mice than wild-type mice, which was also consistent with the increase in viral loads. These results suggest that *C1qa* deficiency enhances susceptibility to MHV A59 systemic infection in mice. This hypothesis is consistent with previous studies reporting that *C1qa*-deficient mice were more susceptible than wild-type mice after both intranasal and intraperitoneal inoculation with *Streptococcus pneumoniae* [12] as well as intraperitoneal and intravenous infection with *Salmonella enterica* serovar Typhimurium [19].

To better understand the immunopathogenesis of MHV A59 infection, we investigated the mRNA expression levels of cytokines and chemokines in the spleen. We observed that *C1qa*-deficient mice had higher IFN- γ , MIP-1 α , and MCP-1 expression in comparison to wild-type mice on day 6 after MHV A59 infection. These proinflammatory cytokines and chemokines play a key role in the inflammatory response. During sepsis, unbalanced inflammatory response to infection has been found to contribute to the pathogenesis of multiple organ failure [20,21]. Previous studies have revealed that IFN- γ is essential to the development of coronaviral hepatitis in mice after MHV A59 infection [22,23], which is consistent with the increased abundance of IFN- γ in response to MHV A59 infection in this study. MIP-1 α plays an important

role in the inflammatory response to viral infection [24-26], and MCP-1 regulates the migration of monocytes, T lymphocytes, and natural killer cells [27]. As seen in previous results [23,28], the expression levels of MIP-1 α and MCP-1 were significantly enhanced in *C1qa* KO mice, which were more prone to MHV A59 infection. Based on this cytokine and chemokine data, the increased levels of proinflammatory responses in *C1qa*-deficient mice could explain the increase in susceptibility to MHV A59. Further research is needed to investigate the role of complement system in the pathogenesis of diseases using the viral infection model in *C1qa*-deficient mice.

In summary, our data suggest that susceptibility to MHV A59 is severely enhanced by *C1qa* deficiency, and the classical complement pathway plays an important role in protecting the host against MHV A59 infection.

SUPPLEMENTARY MATERIAL

Supplementary Fig. 1

PCR genotyping of *C1qa*-deficient mice. PCR products for *C1qa*^{-/-} (257 bp) and wild-type (219 bp) mice.

[Click here to view](#)

REFERENCES

1. Fehr AR, Perlman S. Coronaviruses: an overview of their replication and pathogenesis. *Methods Mol Biol.* 2015;1282:1-23.
[PUBMED](#) | [CROSSREF](#)
2. Sutton TC, Subbarao K. Development of animal models against emerging coronaviruses: from SARS to MERS coronavirus. *Virology.* 2015;479-480:247-258.
[PUBMED](#) | [CROSSREF](#)
3. Barthold SW. Olfactory neural pathway in mouse hepatitis virus nasooencephalitis. *Acta Neuropathol.* 1988;76(5):502-506.
[PUBMED](#) | [CROSSREF](#)
4. Otter JA, Donskey C, Yezli S, Douthwaite S, Goldenberg SD, Weber DJ. Transmission of SARS and MERS coronaviruses and influenza virus in healthcare settings: the possible role of dry surface contamination. *J Hosp Infect.* 2016;92(3):235-250.
[PUBMED](#) | [CROSSREF](#)
5. Homberger FR, Zhang L, Barthold SW. Prevalence of enterotropic and polytropic mouse hepatitis virus in enzootically infected mouse colonies. *Lab Anim Sci* 1998;48(1):50-54.
[PUBMED](#)
6. Stoermer KA, Morrison TE. Complement and viral pathogenesis. *Virology.* 2011;411(2):362-373.
[PUBMED](#) | [CROSSREF](#)
7. Rus H, Cudrici C, Niculescu F. The role of the complement system in innate immunity. *Immunol Res.* 2005;33(2):103-112.
[PUBMED](#) | [CROSSREF](#)
8. Taylor PR, Carugati A, Fadok VA, Cook HT, Andrews M, Carroll MC, et al. A hierarchical role for classical pathway complement proteins in the clearance of apoptotic cells in vivo. *J Exp Med.* 2000;192(3):359-366.
[PUBMED](#) | [CROSSREF](#)
9. Botto M, Dell'Agnola C, Bygrave AE, Thompson EM, Cook HT, Petry F, et al. Homozygous C1q deficiency causes glomerulonephritis associated with multiple apoptotic bodies. *Nat Genet.* 1998;19(1):56-59.
[PUBMED](#) | [CROSSREF](#)
10. Chi S, Yu Y, Shi J, Zhang Y, Yang J, Yang L, et al. Antibodies against C1q are a valuable serological marker for identification of systemic lupus erythematosus patients with active lupus nephritis. *Dis Markers.* 2015;2015:450351.
[PUBMED](#) | [CROSSREF](#)

11. Korb LC, Ahearn JM. C1q binds directly and specifically to surface blebs of apoptotic human keratinocytes: complement deficiency and systemic lupus erythematosus revisited. *J Immunol* 1997;158(10):4525-4528.
[PUBMED](#)
12. Brown JS, Hussell T, Gilliland SM, Holden DW, Paton JC, Ehrenstein MR, et al. The classical pathway is the dominant complement pathway required for innate immunity to *Streptococcus pneumoniae* infection in mice. *Proc Natl Acad Sci U S A*. 2002;99(26):16969-16974.
[PUBMED](#) | [CROSSREF](#)
13. Lee H, Kim JI, Park JS, Roh JI, Lee J, Kang BC, et al. CRISPR/Cas9-mediated generation of a *Plac8* knockout mouse model. *Lab Anim Res*. 2018;34(4):279-287.
[PUBMED](#) | [CROSSREF](#)
14. Ma L, Chung WK. Quantitative analysis of copy number variants based on real-time LightCycler PCR. *Curr Protoc Hum Genet*. 2014;80(1):21.
[PUBMED](#) | [CROSSREF](#)
15. Li G, Fan Y, Lai Y, Han T, Li Z, Zhou P, et al. Coronavirus infections and immune responses. *J Med Virol*. 2020;92(4):424-432.
[PUBMED](#) | [CROSSREF](#)
16. Miura TA, Travanty EA, Oko L, Bielefeldt-Ohmann H, Weiss SR, Beauchemin N, et al. The spike glycoprotein of murine coronavirus MHV-JHM mediates receptor-independent infection and spread in the central nervous systems of *CeacamLa⁺* Mice. *J Virol*. 2008;82(2):755-763.
[PUBMED](#) | [CROSSREF](#)
17. Navas S, Seo SH, Chua MM, Das Sarma J, Lavi E, Hingley ST, et al. Murine coronavirus spike protein determines the ability of the virus to replicate in the liver and cause hepatitis. *J Virol*. 2001;75(5):2452-2457.
[PUBMED](#) | [CROSSREF](#)
18. Walsh KB, Edwards RA, Romero KM, Kotlajich MV, Stohlman SA, Lane TE. Expression of CXC chemokine ligand 10 from the mouse hepatitis virus genome results in protection from viral-induced neurological and liver disease. *J Immunol*. 2007;179(2):1155-1165.
[PUBMED](#) | [CROSSREF](#)
19. Warren J, Mastroeni P, Dougan G, Noursadeghi M, Cohen J, Walport MJ, et al. Increased susceptibility of C1q-deficient mice to *Salmonella enterica* serovar Typhimurium infection. *Infect Immun*. 2002;70(2):551-557.
[PUBMED](#) | [CROSSREF](#)
20. Ding R, Meng Y, Ma X. The central role of the inflammatory response in understanding the heterogeneity of sepsis-3. *BioMed Res Int*. 2018;2018:5086516.
[PUBMED](#) | [CROSSREF](#)
21. Nedeva C, Menassa J, Puthalakath H. Sepsis: inflammation is a necessary evil. *Front Cell Dev Biol*. 2019;7:108.
[PUBMED](#) | [CROSSREF](#)
22. Kim KD, Zhao J, Auh S, Yang X, Du P, Tang H, et al. Adaptive immune cells temper initial innate responses. *Nat Med*. 2007;13(10):1248-1252.
[PUBMED](#) | [CROSSREF](#)
23. Schijns VE, Haagmans BL, Wierda CM, Kruihof B, Heijnen IA, Alber G, et al. Mice lacking IL-12 develop polarized Th1 cells during viral infection. *J Immunol* 1998;160(8):3958-3964.
[PUBMED](#)
24. Cook DN, Beck MA, Coffman TM, Kirby SL, Sheridan JF, Pragnell IB, et al. Requirement of MIP-1 alpha for an inflammatory response to viral infection. *Science*. 1995;269(5230):1583-1585.
[PUBMED](#) | [CROSSREF](#)
25. Domachowske JB, Bonville CA, Gao JL, Murphy PM, Easton AJ, Rosenberg HF. The chemokine macrophage-inflammatory protein-1 alpha and its receptor CCR1 control pulmonary inflammation and antiviral host defense in paramyxovirus infection. *J Immunol*. 2000;165(5):2677-2682.
[PUBMED](#) | [CROSSREF](#)
26. Glass WG, Rosenberg HF, Murphy PM. Chemokine regulation of inflammation during acute viral infection. *Curr Opin Allergy Clin Immunol*. 2003;3(6):467-473.
[PUBMED](#) | [CROSSREF](#)
27. Deshmane SL, Kremlev S, Amini S, Sawaya BE. Monocyte chemoattractant protein-1 (MCP-1): an overview. *J Interferon Cytokine Res*. 2009;29(6):313-326.
[PUBMED](#) | [CROSSREF](#)
28. Maelfait J, Roose K, Vereecke L, Mc Guire C, Sze M, Schuijs MJ, et al. A20 deficiency in lung epithelial cells protects against influenza A virus infection. *PLoS Pathog*. 2016;12(1):e1005410.
[PUBMED](#) | [CROSSREF](#)